Waves Generated During Electron Beam Emissions From The Space Shuttle

T. Neubert,[1] W. W. L. Taylor,[2] L. R. O. Storey,[1] N. Kawashima,[3] W. T. Roberts,[4] D. L. Reasoner,[4] P. M. Banks,[1] D. A. Gurnett,[5] R. L. Williams,[6] and J. L. Burch[6]

Some results from the SEPAC (Space Experiments with Particle Accelerators) experiment flown on the Spacelab 1 shuttle mission are presented. The active part of the experiment included the injection of electron beams at currents up to 300 mA, and energies up to 5 keV. The main focus of the paper is on the wave activity observed during these beam emissions. It is found that the noise in the 0.75- to 10-kHz VLF band has a spectral shape that can be characterized by an f^{-n} law, and that the VLF signal level depends on the beam angle to the magnetic field, the strongest emissions being observed for parallel beams. These features are found to be consistent with a drift wave instability. In the 0.1- to 8-MHz frequency range, very little activity is detected, probably due to a too low gain setting. Reference is made to results from two other electron beam experiments performed from the space shuttle, namely PICPAB (Phenomena Induced by Charged Particle Beams), also flown on Spacelab 1, and FPEG (Fast Pulse Electron Gun) flown on STS 3. Some comments on the space shuttle as a platform for investigation of beam-plasma interactions are provided.

1. INTRODUCTION

Beams of electrons injected into the ionosphere and magnetosphere from spacecraft can be used as diagnostic tools to help answer major questions in the plasma physics of those regions. It is possible with this technique to map magnetic field lines, probe electric potential distributions, study the dynamics of aurora by creating artificial auroras, etc. The local electric field, for instance, is probed by injecting an electron beam perpendicular to the earth's magnetic field as was done on the GEOS 1 and GEOS 2 satellites [Melzner et al., 1978; Junginger et al., 1984] while the potential distributions on a more global scale can be probed for smaller beam angles by either observing the beams at large distances from the spacecraft, or, since the beam electrons are mirrored in the earth's magnetic field, by observing the echo received on the spacecraft itself. See the reviews by Winckler [1980, 1982], and Annales de Géophysique [1980], which devotes an entire issue to the results of the Artificial Radiation and Aurora between Kerguelen and the Soviet Union (ARAKS) rocket experiment.

Beams in plasmas may also generate a wealth of plasma physical phenomena. The beam itself is subject to electrostatic expansion and subsequent stabilization by ion pickup. Depending on the beam energy and current, waves with frequencies at least up to the upper hybrid resonance, with amplitudes of the order of V/m, can be stimulated. These waves destroy the beam by scattering the electrons in pitch angle and energy and constitute a problem for experimenters probing the large scale features of the magnetosphere.

However, the instabilities thus generated are interesting in themselves, as beams occur naturally in space. Examples are energetic electrons accelerated down the magnetic field lines of the earth, exciting aurora as they hit the upper atmosphere, or streams of plasma injected from the sun during solar flares. A controlled experiment can then lead to a deeper understanding of some of the basic plasma physical processes occurring in the universe.

One problem frequently encountered is that the beam-emitting spacecraft charges, if the surrounding plasma is unable to provide a sufficient return current to the spacecraft. In the case of the Space Experiments with Particle Accelerators experiment (SEPAC), the shuttle may at times have charged to the beam potential for currents larger than 100 mA [Sasaki et al., 1986]. This charging affects the beam propagation and influences the plasma diagnostics measurements, because these are disturbed by sheath effects. Another phenomenon is that of beam plasma discharge (BPD). If sufficient neutral gas is present, which is the case at least in the lower part of the ionosphere, the beam may cause a cascadelike ionization of the neutral gas. This is an explosive instability called BPD [Bernstein et al., 1979; Rowland et al., 1981]. While BPD may be viewed as an obstacle for experimenters, it may also, once it is more thoroughly understood, be used as a means for controlling the potentials of ionospheric spacecraft. Applications of artificial particle beams in space plasma studies are discussed in the work by Grandal [1982].

This paper presents observations, from the November 1983 SEPAC experiment on the Spacelab 1 (SL 1) shuttle mission, of waves generated during electron beam emissions. The SEPAC experiment was designed to probe the ionosphere and magnetosphere, to study beam-plasma interactions, and to study the experimental aspects of emitting beams from spacecraft. The dependence of the wave intensity on the beam parameters and the shuttle attitude is out-

---

[1] STAR Laboratory, Stanford University, Stanford, California.

[2] TRW, Redondo Beach, California.

[3] The Institute of Space and Astronautical Science, Tokyo, Japan.

[4] Marshall Space Flight Center, Huntsville, Alabama.

[5] Department of Physics and Astronomy, University of Iowa, Iowa City, Iowa.

[6] Southwest Research Institute, San Antonio, Texas.

lined, and the shapes of the wave spectra are discussed. The experimental sequence analyzed is called Functional Objective 2 (FO-2). A more general description of observations during this sequence is given by *Sasaki et al.* [1986] and *Taylor et al.* [1985].

The SEPAC observations are viewed in a broader context by comparing them with observations from two similar experiments also flown on the space shuttle. The first of these is Phenomena Induced by Charged Particle Beams (PIC-PAB) which was part of the SL 1 mission. The experiment included charged particle accelerators, and various diagnostic instruments. Thus, signals from the SEPAC experiments were recorded by the PICPAB probes and vice versa. A description of the PICPAB experiment and some results are given by *Beghin et al.* [1984] and references therein.

The second experiment is the Vehicle Charging and Potential (VCAP) experiment, which was part of the STS 3 shuttle mission. The VCAP experiment included a series of dc electron beam firings from the Fast Pulse Electron Gun (FPEG) of March 1982. The response of the plasma was probed by the plasma diagnostics package (PDP). Some results and a description of the experiments are found in the works by *Shawhan et al.* [1984a, b], *Banks et al.* [1986], and references therein.

Section 2 contains a description of SEPAC and of the experimental conditions. In section 3, the observations are presented, while section 4 contains a discussion and some concluding remarks.

2. THE SEPAC EXPERIMENT

Spacelab 1 was launched on November 28, 1983, into an orbit with 57° inclination and 240 km altitude. The SEPAC system consisted of the electron beam accelerator (EBA), the magneto plasma dynamic arcjet (MPD), the neutral gas plume ejector (NGP), the diagnostics package (DGP) and the monitor television camera (MTV). The configuration when mounted in the shuttle bay is shown in Figures 1a and 1b along with the shuttle coordinate system. The z axis points toward the nose of the shuttle. The characteristics of the accelerators and the diagnostics are given by *Obayashi et al.* [1982]. Here we shall only describe the part of the experiment that is relevant for the wave observations.

The experimental sequence of electron beam emissions called FO-2 is shown in Figure 2. In all, 45 pulses were injected during a 15-min time period. The pulse length was 5 s for the first 18 pulses, and 1 s for the rest. The accelerator included a focusing coil, creating a pencil-shaped beam. The beam could be deflected up to 30° from the negative direction of the z axis and had an initial diameter of about 2 cm.

The response of the plasma was probed by the DGP and MTV. The DGP included a Langmuir probe, electron spectrum analyzers, a floating probe, a photometer, and two monopole antennas for the detection of the electric component of waves up to 8 MHz. The high-frequency part of the antenna was a 435-mm-long, 30-mm-diameter cylinder, which also served as the shaft on which the Faraday Cup was mounted. The outer shell of the Faraday Cup served as a low-frequency antenna. The signals from the probe were fed to a low-frequency receiver with a 750-Hz to 10-kHz passband, and to a high-frequency receiver, which selected alternately a 100-kHz to 4-MHz band, or a 4.1-MHz to 8-

MHz band. The amplifiers had two possible gains, high and low, with a 40-dB automatic gain control (AGC) dynamic range within each. During the FO-2 sequence the amplifiers were in low gain.

The analog signals from the receivers were recorded on video tape on board the space shuttle. On the ground, the 4-MHz bandwidth HF signal was split into five separate bands roughly 1 MHz wide and heterodyned down to below 1 MHz, in order to ease the later data analysis.

While the AGC level of the VLF receiver is presently available for 42 out of 45 pulses, the actual analog signal is only recorded when the HF receiver is observing in the lower 4-MHz band. This was the case for 24 pulses.

During the 15-min duration FO-2 sequence described here, the velocity vector was almost constant in the shuttle reference frame with the bay of the shuttle (containing the experiments) being in the wake, and the surrounding plasma flowing relative to the shuttle from below the starboard wing with a speed of approximately 7 km/s. The beam pitch angle to the magnetic field first decreased from 21° to 2.5°, and later increased again, reaching 68.5° at the end of the sequence.

The wake structure was also fairly constant at this time, and the angle between the magnetic field and the velocity vector varied by only 20°, from 138° to 118°. The experiment was performed during nighttime and is unique in the sense that all important attitude parameters had very small variations, except for the angle of the magnetic field as defined in the shuttle reference frame.

3. EXPERIMENTAL RESULTS

HF Wave Observations During Beam Emissions

Activity in the 100-kHz to 8-MHz frequency range was detected during three pulses, pulses 20, 22, and 24, which are also the pulses generating the strongest VLF noise. Due to limitations in the signal processing equipment, only the 100-kHz to 600-kHz range of each of the five 0.1-MHz to 1-MHz frequency bands has been analyzed. However, activity is only observed in the lowest band and is at the noise level for frequencies between 500 and 600 kHz.

The frequency-time spectrum observed during the strongest pulse, the 1-s pulse 20, is shown in Figure 3. The beam energy and current are 4.9 keV and 104 mA respectively, and the beam pitch angle is 4°.

The strong emissions below 10 kHz are intense waves detected by the VLF experiment, which are recorded on the same track of the magnetic tape. The HF spectral density decreases with increasing frequency and fluctuates somewhat in time, with an approximately 100-ms period. It is not yet established whether this fluctuation is real or an instrumental effect. The spectra of pulses 22 and 24 have the same characteristics.

Plasma waves from 0.1 to 8 MHz were not observed for the majority of the pulses, probably due to the low gain setting of the amplifier during this sequence. However, the PICPAB experiment (0.1–11.2 MHz) did measure wave activity up to 5 MHz during SEPAC electron beam emissions [*Beghin et al.*, 1984], primarily at the harmonics of the electron gyrofrequency. On the STS 3 mission, the FPEG electron beams (100 mA, 1 keV) generated wave activity, observed by the PDP, at the electron gyrofrequency and the upper hybrid frequency [*Shawhan et al.*, 1984b].
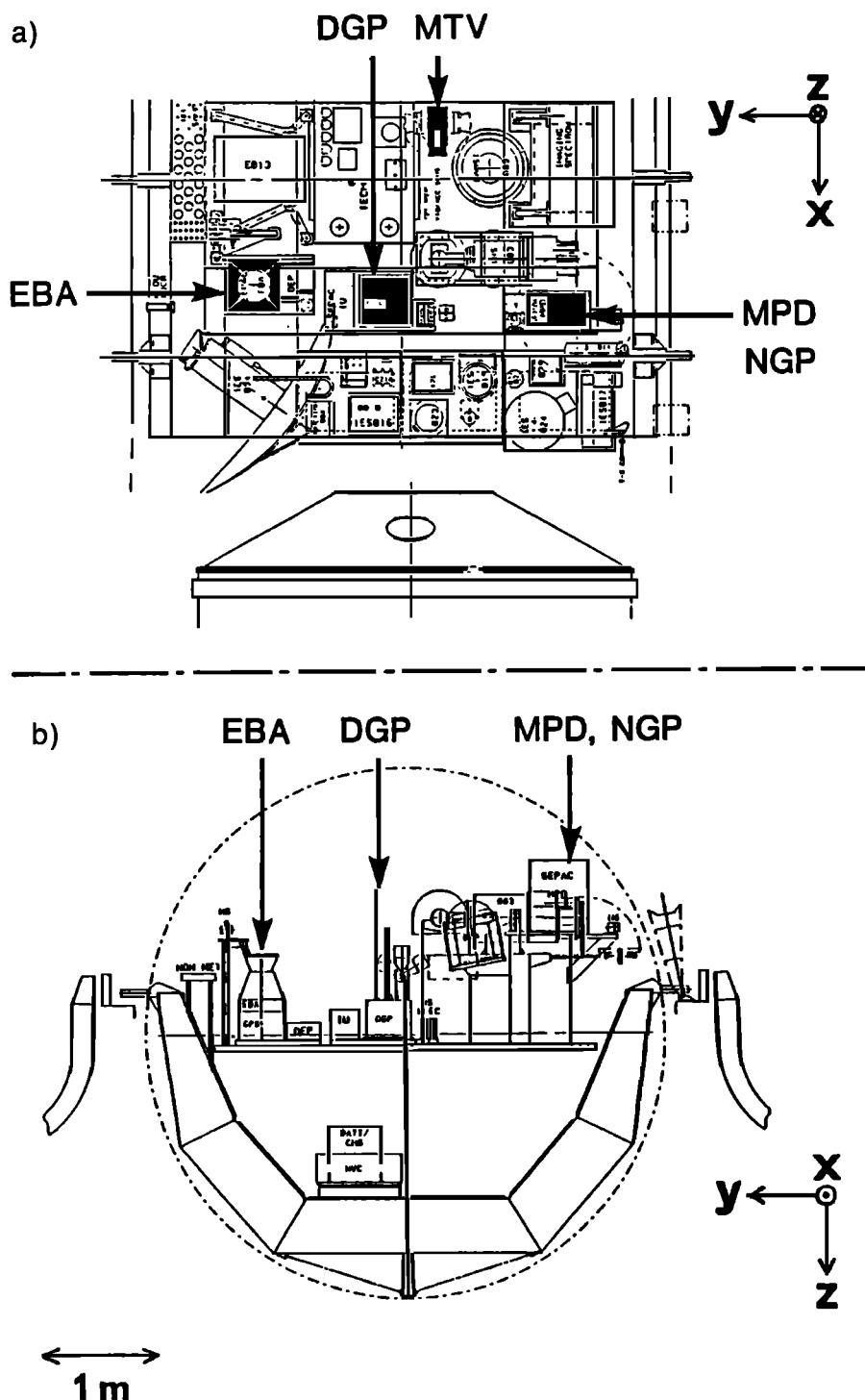
Fig. 1. Configuration of the SEPAC instruments on the Spacelab pallet.

VLF Spectral Shape During Beam Emissions

During the electron beam emissions of SEPAC, strong wave activity is always observed in the 750-Hz to 10-kHz VLF range. The spectral density of the amplitude of the electric field noise is proportional to f^{-n}, with n varying from 0.7 for the stronger pulses to 1.5 for the weaker pulses. Two examples of amplitude spectra obtained for the strongest pulse, pulse 20, and pulse 37 are shown in Figure 4.

The spectra do show some smaller variations though, and a classification has been done [Akai, 1984]. Such a classification is of interest because laboratory plasma chamber experiments show that the VLF spectrum obtained during electron beam emissions is radically different for pre-BPD conditions, than in the presence of BPD [Holtzworth et al., 1982]. Well below the BPD threshold, the spectra are similar to the SEPAC spectra, while the peak amplitude of the electric noise shifts to higher frequencies close to and above the BPD threshold.
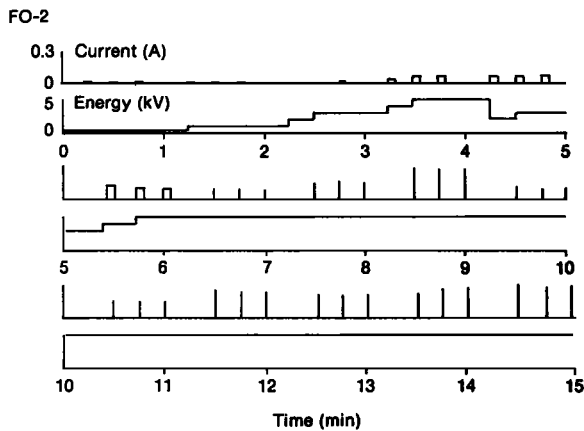
Fig. 2.   Chart of the FO-2 electron beam sequence.

However, one has to be very cautious when interpreting the details of the spectral shape, because they often depend on the wave background activity. This has been found by examining spectra from the PDP obtained during FPEG beams. Figures 5a and 5b show two examples of PDP spectra in the 0- to 10-kHz frequency range; Figure 5a is for the electric field and Figure 5b for the the magnetic. In Figure 5a, an interference line is present just before the beam emission. This line is amplified during the emission and appears in the spectrum even though the AGC gain is reduced by 20 dB during the beam emission. Figure 5b shows the enhancement at and above the lower hybrid resonance (LHR), and the lower cutoff at this resonance, at a time when natural electromagnetic whistler mode wave activity was prominent. The change in signal level during the beam emission compared to no beam emission is in this case less than 1 dB. The observation that the VLF wave spectrum obtained during beam emissions depends on the wave background activity is also mentioned by Denig [1982], who reports on chamber test results for the FPEG/PDP.

The VLF receiver was in low gain during all the active sequences of SEPAC and was too insensitive to detect the background wave intensity. However, we do have data with the receiver in high gain for a few short time intervals during one of the passive FO-13 sequences. An example of the wave spectra received during this sequence is shown in Figure 6a. The narrow-band constant-frequency lines with roughly 1-kHz separation, and the rapidly varying narrow-band emissions seen in the latter half of the spectrogram, appear to be interference lines from the various other electronics on the shuttle. At present they are still unidentified.

The same type of interference pattern is detected about 20% of the time by the VLF plasma wave instrument on the PDP, which was flown on the STS 3 shuttle mission, and continuously monitored the wave activity. An example of the electric field noise spectrum is shown in Figure 6b.

While the spectra in Figures 5 and 6 have been chosen because of their special characteristics, the general picture from the VCAP/PDP observations is that of strong, predominantly electrostatic, VLF activity during dc electron beam emissions, with a wave activity decreasing with increasing frequency. During beam emissions, the electric signal rises up to 40 dB above the background noise level, while the magnetic signal level only increases by a few dB.

VLF Signal Intensity During Beam Emissions

Figure 7 shows the variation of the signal strength as measured by the AGC level as a function of the beam pitch angle θ. The average AGC level for each pulse is plotted so that the first pulses emitted show up to the left in the figure, when the pitch angle in general was decreasing, and the last pulses to the right, when the pitch angle was increasing again. In the figure, strong signals have positive AGC levels. Also indicated are the points corresponding to 8-, 24-, 56- and 72-mA currents. Table 1 lists the signal level, beam pitch angle and beam parameters for the low current and low energy pulses emitted in the beginning of the sequence.

From Figure 7, it can be seen that the signal level depends on the beam current I_B and energy V_B and on the beam pitch angle θ. For low currents and energies the VLF emission intensity is low, while for currents larger than 78 mA it varies smoothly with pitch angle, reaching a maximum at $\theta = 0°$. It is not possible to establish a more detailed functional relationship of the signal level with beam current and energy for the low current pulses as this relationship is masked by the pitch angle dependence. The apparent saturation of the wave activity at about 100-mA beam currents correlates with the spacecraft potential which has been reported to reach the beam energy for currents larger than 100 mA [Sasaki et al., 1986].

With currents above 100 mA, the electric field signal level decreases by 20 dB from the smallest pitch angles to the larger pitch angles. This indicates that the wave signal intensity has a true dependence on the beam angle. As we have mentioned earlier, the pitch angle is the only parameter with a significant (to our knowledge) variation during this sequence. Also, the noise level is fairly constant for pitch angles larger than 20°. This may explain why the same effect is not observed in the VCAP/PDP experiment on STS 3, where the minimum angle obtained during dc beam emissions was 28°.

4. DISCUSSION

Probably the most interesting aspect of the VLF wave emissions observed during the beam firings is the variation of the wave intensity with beam pitch angle. While beam-generated ELF-VLF emissions have been observed on nu-
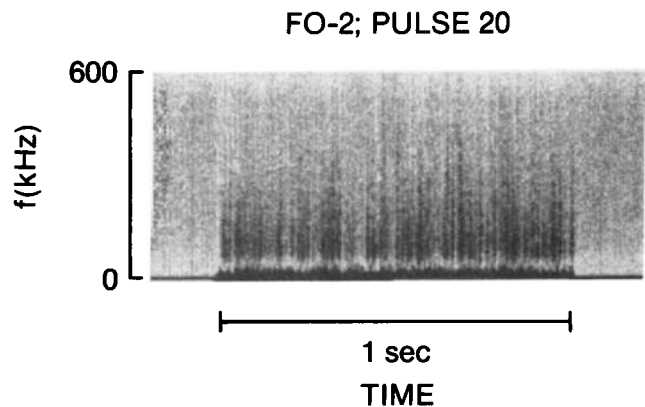
FO-2; PULSE 20

Fig. 3.   Frequency-time spectrogram of 100- to 600-kHz wave emissions during the 1-s duration pulse 20, strong signals appearing dark. $I_b = 104$ mA, $V_b = 4.9$ keV, $\theta = 4°$. The signals below 10 kHz are from the VLF instrument recorded on the same track.

SEPAC

PULSE 20: $\theta = 4°$
$V_B = 4900V$, $I_B = 104mA$

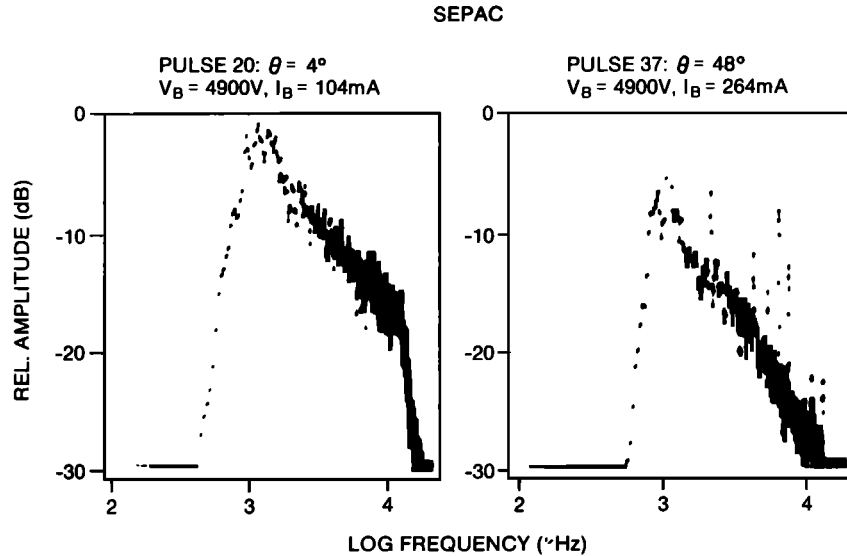PULSE 37: $\theta = 48°$
$V_B = 4900V$, $I_B = 264mA$

Fig. 4. Spectra of signal amplitude during pulse 20 and pulse 37.

merous occasions both from spacecraft and in space simulation chamber experiments, their relation to the pitch angle has to our knowledge only been explored during the Electron Echo 1 rocket experiment for pitch angles between 70° and 110° [Cartwright and Kellogg, 1974]. In the following we will discuss this feature and the instability likely to generate the VLF turbulence.

There is now some evidence that beam-generated ELF-VLF turbulence observed in space simulation chambers and from rockets can be caused by a drift wave instability [Walker and Szuszczewicz, 1985; Winckler et al., 1985]. This instability relies on the existence of gradients in the plasma density (and/or the temperature) [Hasegawa, 1971; Cap, 1976; Chen, 1984], which conceivably are created by the electron beam. The waves are generally assumed to have wave normals k almost perpendicular to the magnetic field, with a small but finite parallel component $k_\parallel$. Drift waves may for instance propagate in the azimuthal direction around the beam with a velocity of the order of the electron diamagnetic drift velocity V_D as suggested by Walker and Szuszczewicz [1985] reporting on observations of electrostatic wave turbulence during a space simulation BPD. However, the instability does not rely on the presence of the beam itself or on a cylindrical geometry. Thus, naturally occurring ELF turbulence in the equatorial ionosphere associated with spread F is thought to be the result of a drift wave instability [Kelley, 1982]. A review of drift wave instabilities can be found in the work by Cap [1976].

The instability is also discussed by Yamada and Hendel [1978]. They find that a negative radial gradient in the ion or electron temperature created by the beam can destabilize the system and create a continuous-spectrum instability for frequencies $f_{ci} < f < f_{pi}$, where f_{ci} and f_{pi} are the ion gyrofrequency and plasma frequency. The growth rate can be as large as f_{ci}, and the frequency with the maximum amplitude is proportional to $\sqrt{n_e}$, where n_e is the electron density. In the ionosphere at the 240-km altitude of the shuttle, the major ion constituent is O^+, and f_{ci} is typically $\simeq 40$ Hz and $f_{pi} \simeq 16$ kHz.

In experiments performed in space simulation chambers,

it is found that the BPD is ignited when the electron density reaches a threshold which in terms of the electron plasma frequency f_{pe} and gyrofrequency f_{ce} can be expressed as $f_{pe} \simeq 6 f_{ce}$ [Walker et al., 1982; Szuszczewicz et al., 1982], and that the electron density increases by a factor of two to three when BPD is ignited [Walker et al., 1982]. The observations of Holtzworth et al. [1982] that the maximum of the VLF spectra is shifted to higher frequencies as the BPD threshold is reached is then in qualitative agreement with the predictions of drift wave turbulence.

In The work by Chen [1965], a different approach is taken. It is observed that drift wave spectra generated in entirely different devices are strikingly similar for an intermediate range of k values, where the small-k end of the spectrum is dependent on the dimension of the system and the large-k end on the electron Larmor radius, which determines the lowest possible wavelengths for drift waves. This was used together with dimensional arguments to show that the fluctuations in the potential $\tilde{\varphi}^2$ are proportional to k^{-5}. For drift waves the electrons are assumed to follow the Boltzmann equation as electrons can stream along the magnetic field line ($k_\parallel$ finite). On the other hand, the parallel wavelength is assumed to be so large that the electrons cannot completely short-circuit the potential variations. The fluctuations in electron density $\tilde{n}_e^2$ are then also proportional to k^{-5}, as $\tilde{n}_e/n_e \simeq e\tilde{\varphi}/KT_e$, where K is Boltzmann's constant, e the electron charge and T_e the electron temperature. The electric field fluctuations $\tilde{E}$ relate to the potential fluctuations through $\tilde{E} \simeq ik\tilde{\varphi}$, and thus power spectra of the electric field are proportional to k^{-3}. The phase velocity of the drift waves is constant and equals the diamagnetic drift velocity V_D. It then follows that the slope of spectra on a log-log scale is independent of whether the fluctuations are plotted as a function of k or f.

Turning to the SEPAC observations, we note that the spectra shown in Figure 4 are spectral density of electric field amplitude versus frequency. For drift waves, we would expect the spectral density to be roughly proportional to f^{-n}, with $n = 1.5$. This functional dependency of f fits the data very well, especially for the lower amplitude waves. We

FPEG/PDP

a) ELECTRIC   BEAM

b) MAGNETIC

NO BEAM

BEAM
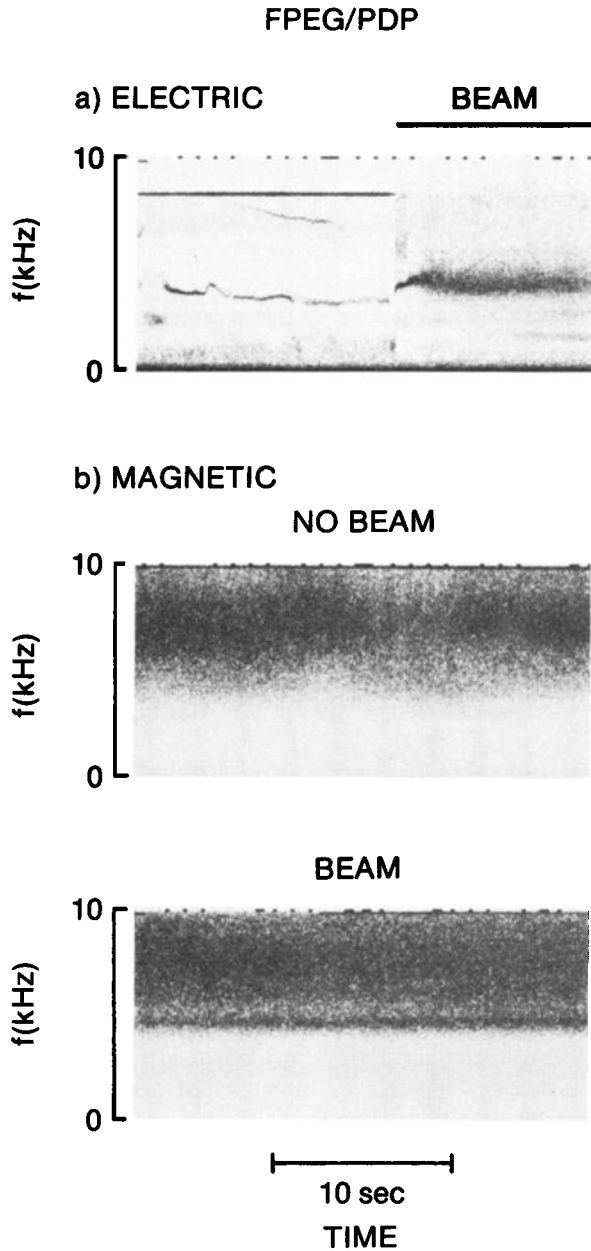

⊢————————⊣
10 sec
TIME

Fig. 5. Influence of the ambient noise on the VLF spectral shape observed during FPEG/PDP electron beam emissions: (a) 0–10 kHz electric, (b) 0–10 kHz magnetic.

note here that since $2\pi f \simeq kV_D$, the slope of a spectrum is not affected by Doppler shifts induced by the shuttle motion or the rotational **E x B** drifts caused by the radial electric field associated with the beam.

We now explore whether the SEPAC electron beams create sufficient enhancement of the ambient electron density around the beam to support a drift wave instability. We will first estimate the maximum electron density n_m created through beam electron-neutral gas collisions for a beam pitch angle $\theta = 0°$. It is approximately given by

$$n_m \simeq \gamma t_m \tag{1}$$

The ionization rate γ and the maximum time t_m that a volume element of neutral gas is exposed to the beam are

$$\gamma = I_B n_n \sigma / eA \tag{2}$$

$$t_m = d/V_s \tag{3}$$

Here, I_B is the beam current, n_n is the neutral gas density, σ the ionization cross section, A the beam cross section, d the beam diameter and V_s the shuttle velocity perpendicular to the earth's magnetic field.

The neutral gas pressure measured in the shuttle bay during the FO-2 sequence is $\simeq 5 \times 10^{-6}$ torr corresponding to $n_n \simeq 5 \times 10^{10}$ cm^{-3}. For the beam energy $V_B \simeq 1$ keV, $\sigma \simeq 2 \times 10^{-17}$ cm^2 for O and N [*Banks and Kockharts*, 1973]. This gives a free mean path $\lambda_m = 1/\sigma n_n \simeq 10$ km. Assuming the beam cross section to be $\simeq 100$ cm^2 and the beam current to be 160 mA, we find $\gamma \simeq 10^{10}$ cm^{-3} s^{-1}.

As mentioned in section 2, the angle between the magnetic field and the shuttle velocity vector varied during FO-2 from 131° to 111°. As the total shuttle velocity was $\simeq 7$ km/s, a typical value for the perpendicular component V_s is $V_s \simeq 3.3$ km/s. Estimating the beam diameter to be $d \simeq 10$ cm, we find $t_m \simeq 3 \times 10^{-5}$ s.

The maximum electron density produced by beam electron collisions with the neutral gas is with these assumptions $\simeq 3 \times 10^5$ cm^{-3} which is $\simeq 3$ times larger than the expected ambient electron density during the FO-2 nighttime sequence.

In (1), the loss of electrons due to diffusion perpendicular to the magnetic field line has been neglected. Assuming the loss term to be of the form $\simeq n_e/\tau$ where τ is a characteristic time constant, this is valid for $t_m \ll \tau$. For a cylindrical column of diameter d the time constant τ_B for Bohm diffusion is $\tau_B = d^2/8D_B$. The Bohm diffusion coefficient $D_B = v_{is}^2/$

a)   SEPAC

⊢————————⊣
10 sec
TIME

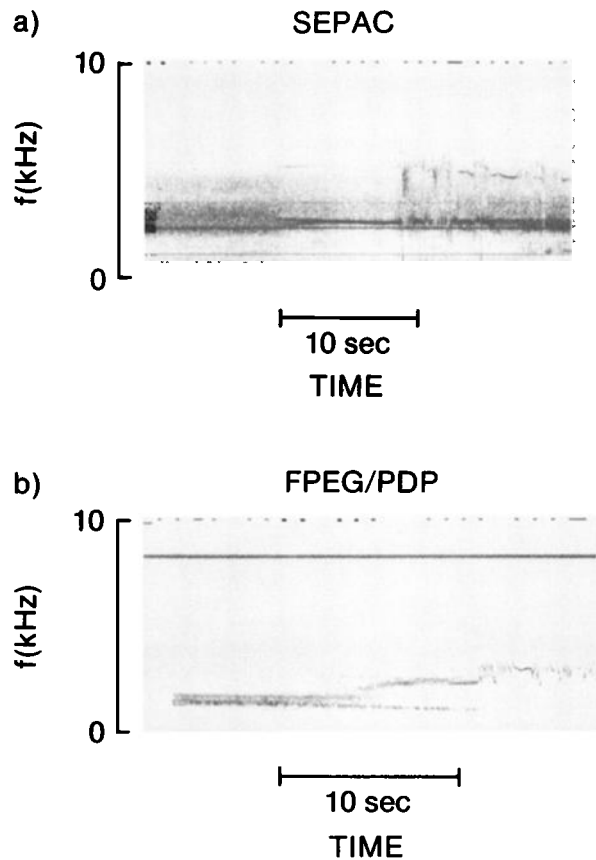### b)   FPEG/PDP

⊢————————⊣
10 sec
TIME

Fig. 6. Gray scale spectrograms of the 0- to 10-kHz ambient electric shuttle noise, strong signals appearing dark: (a) SEPAC (b) FPEG/PDP.

$(32\pi f_{ci})$ where v_{is} is the ion sound velocity. For the experimental conditions typical values of v_{is} and f_{ci} are $v_{is} \simeq 10^3$ m/s and $f_{ci} \simeq 40$ Hz. A 10-cm-diameter column then has the Bohm time $\tau_B \simeq 5 \times 10^{-6}$ s.

The classical diffusion coefficient perpendicular to the magnetic field $D_\perp$ in a weakly ionized gas can be expressed as $D_\perp/D_B = 16\nu_n/f_{ce}$ where ν_n is the electron-neutral gas collision frequency. At the shuttle altitude $\nu_n \simeq 10^2$ Hz and $f_{ce} \simeq 10^6$ Hz and the classical diffusion coefficient is three orders of magnitude smaller than the Bohm diffusion coefficient. Thus, (1) is a good approximation if the diffusion is classical. We would then expect large gradients in the electron density in the direction of the shuttle velocity component perpendicular to the magnetic field, as the increase in the density occurs over a short distance, namely the beam diameter d. In fact, the maximum gradients estimated here are about 100 times larger than the ones measured in space simulation chamber experiments during which drift wave turbulence was observed [*Walker and Szuszczewicz*, 1985]. If, however, Bohm diffusion is dominant, as indicated by space simulation chamber experiments [*Szuszczewicz and Lin*, 1982] the gradients are substantially less, and a more rigorous treatment of the problem is needed.

The electrons produced by the beam have energies in the range 5–50 eV and move along the magnetic field lines with velocities of the order of 10^6 m/s (25-eV electrons), primarily toward the shuttle, which is charged to positive potentials. For $\theta > 0°$ we now assume that the electrons created by the beam will be homogeneously distributed on a cylindrical shell with a radius that equals the beam Larmor radius r_L.

It can be shown that the production rate of electrons averaged over a beam gyration is weakly dependent on the beam pitch angle. The production rate per unit length along the field line, however, is proportional to $1/\cos\theta$. Since $r_L \propto 1/\sin\theta$, we find that the beam-created electron density when distributed over the cylindrical shell traced by the spiraling beam is proportional to $1/\sin 2\theta$. Assuming that the VLF signal level is proportional to the enhanced electron density

TABLE 1. VLF Signal Level and Beam Parameters for Low Current Pulses

Pulse	I_b, mA	V_b, keV	AGC, dB	θ, deg
1	8	0.34	-25.0	11.0
2	8	0.34	-25.0	7.5
3	8	0.34	-25.0	7.5
4	24	0.94	-18.0	21.5
5	24	0.82	-18.0	6.0
6	unstable			45.0
7	8	1.9	-16.5	16.0
8	24	2.9	-6.5	10.0
9	24	2.9	-5.5	10.5
10	56	4.0	-14.0	9.0
11	72	4.9	-18.0	9.0
12	72	4.9	-22.0	9.0
13	72	1.9	-18.0	11.0
14	72	2.9	-21.5	2.5
15	72	2.9	-15.5	3.5

The beam energy is V_b and the beam pitch angle θ. Strong emissions have more positive AGC levels.

created by the beam, we then expect a $1/\sin 2\theta$ dependence. This functional relationship fits very well with the observations as shown in Figure 7.

We then conclude that, as a source of VLF wave emissions, a drift wave instability is a very attractive candidate. It accounts for the observed frequency range of the emissions, their spectral shape, and the variation of the emission amplitudes with beam pitch angle. We have also shown that the magnitude of the gradients is likely to be sufficient to generate strong VLF turbulence.

We have not addressed the influence of the spacecraft potential or fluctuations in the beam itself when created by the beam accelerator. The reason for this is that these generation mechanisms are not sensitive to small variations θ around $\theta = 0°$. However, the charging of the shuttle may affect the saturation level of the wave emissions.

Turning now to the question of whether BPD is generated, we note that the spectral shape of the three strongest wave emissions stimulated by the electron beams is observed up to 500 kHz, with the wave intensity decreasing with frequency. Spectra observed during BPD in space chambers and from rockets have a wave intensity roughly constant up to the electron gyrofrequency, with a sharp upper cutoff at this frequency. At even higher frequencies, waves are generated at the plasma or upper hybrid frequency [*Bernstein et al.*, 1982]. We therefore conclude that BPD in the classical sense as observed in laboratory plasmas was not triggered by the SEPAC beams. This interpretation is also consistent with the spacecraft potential reaching beam energies for currents larger than 100 mA, as a BPD would increase the ambient ionization and thus increase the return current supplied by the plasma.

The lack of BPD is perhaps not surprising considering the large velocity of the shuttle. However, the threshold may almost have been reached. For a nighttime ionosphere, $f_{pe} \simeq 3f_{ci}$. The maximum increase of the electron density due to beam electron-neutral gas collisions is as previously mentioned expected to be a factor of 3. This would lead to $f_{pe} \simeq 5f_{ci}$ in the beam, which is just below the threshold
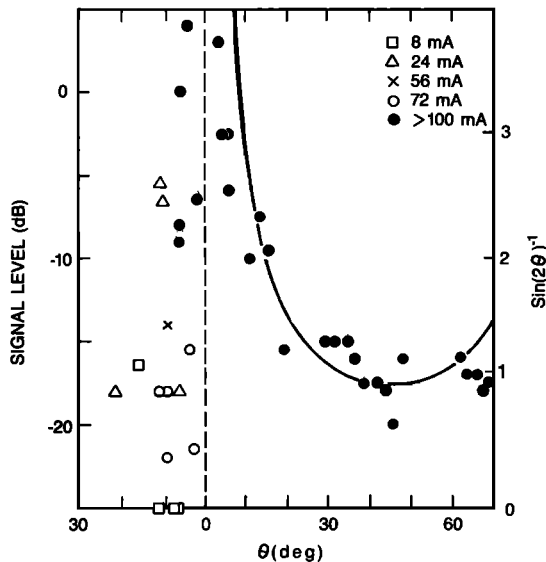

Fig. 7. VLF signal intensity versus beam pitch angle in time sequential order, as measured by the AGC level of the amplifier, and the function $g = 1/\sin 2\theta$ (see text).

for BPD as determined in space simulation chamber experiments.

The space shuttle has proved very useful as a platform for active ionospheric experiments. This is especially the case when the orbit is chosen such that only one of the parameters influencing the investigated interactions is varying. For the study of how the wave generation depends on the beam pitch angle, it was invaluable that all other parameters were constant so that a definite correlation could be established. In the case of the FPEG/PDP experiment, for instance, the VLF signal level stimulated by electron beams varied with orbit attitude. However, it is not easy to decode the observations, as both the magnetic field and the velocity direction varied simultaneously.

From observations of the ambient VLF interference noise of the shuttle (Figure 6), we reach two conclusions. First, the shuttle-generated noise is at a significant level in the sense that it influences the spectral shape of waves generated during beam emissions. Second, the spectral characteristics vary on a time scale of the order of 10 s. Thus, the details of the spectra must be interpreted with caution.

REFERENCES

Akai, K., Electron beam - plasma interaction experiment in space, *Res. Note 285*, Inst. of Space and Astronaut. Sci., Tokyo, 1984. *Annales de Géophysique*, Special issue on the results of the French-Soviet ARAKS experiments, *36*, 271, 1980.

Banks, P. M., and G. Kockharts, *Aeronomy*, Academic, Orlando, Fla., 1973.

Banks, P. M., W. J. Raitt, P. R. Williamson, A. B. White, and R. I. Bush, Results from the vehicle charging and potential experiment on STS-3, *J. Spacecr. Rockets*, in press, 1986.

Beghin, C., J. P. Lebreton, B. N. Maehlum, J. Troim, P. Ingsoy, and J. L. Michau, Phenomena induced by charged particle beams, *Science, 225*, 188, 1984.

Bernstein, W., H. Leinbach, P. J. Kellogg, S. J. Monson, and T. Hallinan, Further laboratory measurements of the beam-plasma discharge, *J. Geophys. Res., 84*, 7271, 1979.

Bernstein, W., P. J. Kellogg, S. J. Monson, R. H. Holzworth, and B. A. Whalen, Recent observations of beam plasma interactions in the ionosphere and a comparison with laboratory studies of the beam plasma discharge, in *Artificial Particle Beams in Space Plasma Studies*, Monograph, edited by B. Grandal, p. 35, Plenum, New York, 1982.

Cap, F. F., *Handbook on Plasma Instabilities*, vol. 1, p. 349, Academic Press, Orlando, Fla., 1976.

Cartwright, D. G. and P. J. Kellogg, Observations of radiation from an electron beam artificially injected into the ionosphere, *J. Geophys. Res., 79*, 1439, 1974.

Chen, F. F., Spectrum of low-β plasma turbulence, *Phys. Rev. Lett., 15*, 381, 1965.

Chen, F. F., *Introduction to Plasma Physics and Controlled Fusion*, vol. 1, Plenum, New York, 1984.

Denig, W. F., Wave and particle observations associated with the beam plasma discharge in a space simulation chamber, Ph.D. thesis, Utah State Univ., Logan, Utah, 1982.

Grandal, B. (Ed.), *Artificial Particle Beams in Space Plasma Studies*, Monograph, Plenum, New York, 1982.

Hasegawa, A., Plasma instabilities in the magnetosphere, *Rev. Geophys., 9*, 703, 1971.

Holtzworth, R. H., W. B. Harbridge, and H. C. Koons, Plasma waves stimulated by electron beams in the lab and in the auroral ionosphere, in *Artificial Particle Beams in Space Plasma Studies*, Monograph, edited by B. Grandal, p. 381 Plenum, New York, 1982.

Junginger, H., G. Geiger, G. Haerendel, F. Melzner, E. Amata, and B. Higel, A statistical study of dayside magnetospheric electric field fluctuations with periods between 150 and 600 s, *J. Geophys. Res., 89*, 5495, 1984.

Kelley, M. C., Nonlinear saturation spectra of electric fields and density fluctuations in drift wave turbulence, *Phys. Fluids, 25*, 1002, 1982.

Melzner, F., G. Metzner, and D. Antrack, The Geos electron beam experiment S 329, *Space Sci. Instrum., 4*, 45, 1978.

Obayashi, T., N. Kawashima, K. Kuriki, N. Nagatomo, K. Ninomiya, S. Sasaki, A. Ushirokawa, I. Kudo, M. Ejiri, W. Roberts, R. Chappell, J. Burch, and P. M. Banks, Space experiments with particle accelerators (SEPAC), in *Artifical Particle Beams in Space Plasma Studies*, Monograph, edited by B. Grandal, p. 659, Plenum, New York, 1982.

Rowland, H. L., C. L. Chang, and K. Papadopoulos, Scaling of the beam-plasma discharge, *J. Geophys. Res., 86*, 9215, 1981.

Sasaki, S., N. Kawashima, K. Kuriki, M. Yanagisawa, T. Obayashi, M. Nagatomo, K. Ninomiya, M. Ejiri, I. Kudo, W. T. Roberts, C. R. Chappell, D. L. Reasoner, J. L. Burch, W. W. L. Taylor, P. M. Banks, P. R. Williamson, and O. K. Garriott, Charge build-up of orbiter measured in SEPAC SPACELAB-1 experiment, *J. Spacecr. Rockets*, in press, 1986.

Shawhan, S. D., G. B. Murphy, and D. L. Fortna, Measurements of electromagnetic interference on OV102 Columbia using the plasma diagnostics package, *J. Spacecr. Rockets, 21*, 392, 1984a.

Shawhan, S. D., G. B. Murphy, P. M. Banks, P. R. Williamson, and W. J. Raitt, Wave emissions from dc and modulated electron beams on STS 3, *Radio Sci., 19*, 471, 1984b.

Szuszczewicz, E. P., and C. S. Lin, Time-dependent plasma behavior triggered by a pulsed electron gun under conditions of beam-plasma-discharge, in *Artificial Particle Beams in Space Plasma Studies*, Monograph, edited by B. Grandal, p. 361, Plenum, New York, 1982.

Szuszczewicz, E. P., K. Papadopoulos, W. Bernstein, C. S. Lin, and D. N. Walker, Threshold criterion for a space simulation beam-plasma discharge, *J. Geophys. Res., 87*, 1565, 1982.

Taylor, W. W. L., T. Obayashi, N. Kawashima, S. Sasaki, M. Yanagisawa, J. L. Burch, D. L. Reasoner, and W. T. Roberts, Wave-particle interactions induced by SEPAC on Spacelab 1: Wave observations, *Radio Sci., 20*, 486, 1985.

Walker, D. N., and E. P. Szuszczewicz, Electrostatic wave observation during a space simulation beam-plasma discharge, *J. Geophys. Res., 90*, 1691, 1985.

Walker, D. N., E. P. Szuszczewicz, and C. S. Lin, Ignition of the beam-plasma-discharge and its dependence on electron density, in *Artificial Particle Beams in Space Plasma Studies*, Monograph, edited by B. Grandal, p. 371, Plenum, New York, 1982.

Winckler, J. R., The application of artificial electron beams to magnetospheric research, *Rev. Geophys., 18*, 659, 1980.

Winckler, J. R., The use of artificial electron beams as probes of the distant magnetosphere, in *Artificial Particle Beams in Space Plasma Studies*, Monograph, edited by B. Grandal, p. 3, Plenum, New York, 1982.

Winckler, J. R., K. N. Erickson, Y. Abe, J. E. Steffen, and P. R. Malcolm, ELF wave production by an electron beam emitting rocket system and its suppression on auroral field lines: Evidence for Alfven and drift waves, *Geophys. Res. Lett., 12*, 457, 1985.

Yamada, M., and H. W. Hendel, Current-driven instabilities and resultant anomalous effects in isothermal, inhomogeneous plasmas, *Phys. Fluids, 21*, 1555, 1978.

P. M. Banks, T. Neubert, and L. R. O. Storey, STAR Laboratory, Durand 331, Stanford University, Stanford, CA 94305.

J. L. Burch and R. L. Williams, Southwest Research Institute, 6220 Culebra Road, San Antonio, TX 78284.

D. A. Gurnett, Department of Physics and Astronomy, University of Iowa, Iowa City, IA 52242.

N. Kawashima, Institute of Space and Astronautical Science, 4-6-1 Komaba, Meguro, Tokyo, 153, Japan.

D. L. Reasoner, Marshall Space Flight Center, Mail Code ES53, Huntsville, AL 35812.

W. T. Roberts, Marshall Space Flight Center, Mail Code PS01, Huntsville, AL 35812.

W. W. L. Taylor, TRW, R1/1170, 1 Space Park, Redondo Beach, CA 90278.